Large-Scale Molecular Comparison of Human Schwann Cells to Malignant Peripheral Nerve Sheath Tumor Cell Lines and Tissues

Shyra J. Miller,[1] Fatima Rangwala,[1] Jon Williams,[1] Peter Ackerman,[1] Sue Kong,[2] Anil G. Jegga,[2] Sergio Kaiser,[2] Bruce J. Aronow,[2] Silke Frahm,[3] Lan Kluwe,[3] Victor Mautner,[3] Meena Upadhyaya,[4] David Muir,[5] Margaret Wallace,[6] Jussara Hagen,[7] Dawn E. Quelle,[7] Mark A. Watson,[8] Arie Perry,[8] David H. Gutmann,[8,9] and Nancy Ratner[1]

Divisions of [1]Experimental Hematology and [2]Biomedical Informatics, Cincinnati Children's Hospital Research Foundation, University of Cincinnati College of Medicine, Cincinnati, Ohio; [3]Department of Neurosurgery, University Clinic Hamburg-Eppendorf, Hamburg, Germany; [4]Institute of Medical Genetics, University of Wales College of Medicine, Heath Park, Cardiff, United Kingdom; Departments of [5]Pediatric Neurology, Neuroscience, and [6]Molecular Genetics and Microbiology, University of Florida, Gainesville, Florida; [7]Department of Pharmacology, University of Iowa College of Medicine, Iowa City, Iowa; and Departments of [8]Pathology and Immunology and [9]Neurology, Washington University School of Medicine, St. Louis, Missouri

Abstract

Malignant peripheral nerve sheath tumors (MPNST) are highly invasive soft tissue sarcomas that arise within the peripheral nerve and frequently metastasize. To identify molecular events contributing to malignant transformation in peripheral nerve, we compared eight cell lines derived from MPNSTs and seven normal human Schwann cell samples. We found that MPNST lines are heterogeneous in their *in vitro* growth rates and exhibit diverse alterations in expression of pRb, p53, $p14^{Arf}$, and $p16^{INK4a}$ proteins. All MPNST cell lines express the epidermal growth factor receptor and lack S100β protein. Global gene expression profiling using Affymetrix oligonucleotide microarrays identified a 159-gene molecular signature distinguishing MPNST cell lines from normal Schwann cells, which was validated in Affymetrix microarray data generated from 45 primary MPNSTs. Expression of Schwann cell differentiation markers (*SOX10, CNP, PMP22*, and *NGFR*) was downregulated in MPNSTs whereas neural crest stem cell markers, *SOX9* and *TWIST1*, were overexpressed in MPNSTs. Previous studies have implicated TWIST1 in apoptosis inhibition, resistance to chemotherapy, and metastasis. Reducing *TWIST1* expression in MPNST cells using small interfering RNA did not affect apoptosis or chemoresistance but inhibited cell chemotaxis. Our results highlight the use of gene expression profiling in identifying genes and molecular pathways that are potential biomarkers and/or therapeutic targets for treatment of MPNST and support the use of the MPNST cell lines as a primary analytic tool. (Cancer Res 2006; 66(5): 2584-91)

Introduction

Malignant peripheral nerve sheath tumors (MPNST) are aggressive soft tissue sarcomas with poor prognosis. Excision of the tumor does not always prevent local recurrence, and metastases to the lung, liver, and brain are common. Current therapeutic regimens have limited use because the tumors are generally resistant to standard chemotherapy and radiation (1). Half of all MPNSTs are sporadic in nature; half arise in individuals with neurofibromatosis type 1 (NF1), an autosomal dominant disorder affecting 1 in 2,500 to 3,500 individuals worldwide (2). MPNSTs represent a major cause of mortality in NF1 patients (3). Nearly all NF1 patients develop benign dermal neurofibromas and ~30% of NF1 patients have benign plexiform neurofibromas (4) which, unlike dermal neurofibromas, can undergo malignant transformation to MPNST (5). Greater than 50% of MPNSTs contain cells immunoreactive for S100β protein, suggesting that tumors arise from neoplastic Schwann cells or their precursors (6).

Human tumor cell lines have historically served as experimental models for the study of tumor cell biology and drug development. A small number of cell lines, derived from NF1-associated MPNSTs (7–10) or sporadic MPNSTs (11, 12), have been reported in the literature but have never been directly compared with each other and primary tumors. These cell lines are a valuable resource as primary MPNSTs are difficult to permanently establish in culture. Here, we used MPNST cell lines to identify differences between MPNST cells and normal human Schwann cells (NHSC), the proposed cell of origin for MPNST.

Molecular events contributing to peripheral nerve tumor development are unclear. In the context of NF1, loss of the *NF1* protein product is believed to be the earliest event as patients inherit a mutated *NF1* allele and lose the second copy in MPNST cells. Loss of *NF1* has also been documented in sporadic cases of MPNST (13). Another early alteration in MPNST development is the expression of epidermal growth factor receptor (EGFR). Whereas EGFR is not expressed in NHSCs, the protein is detected in primary MPNSTs, MPNST cell lines, and subpopulations of neurofibroma Schwann cells (14). Additional genetic mutations targeting regulators of the retinoblastoma protein (pRb) and p53 tumor suppressor pathways seem to represent later events in malignant transformation of Schwann cells as they are not observed in neurofibromas (15–17).

In this study, we identify a gene expression profile that distinguishes MPNST cell lines from NHSCs and validate this MPNST cell line gene signature in a large panel of primary MPNSTs. Furthermore, we provide evidence that one candidate gene overexpressed in all MPNST samples, *TWIST1*, is an attractive therapeutic target for novel MPNST treatment strategies.

Materials and Methods

MPNST tumor acquisition and processing. Tumor specimens and corresponding clinical data were collected and used in accordance with Institutional Review Board–approved protocols. The diagnosis of NF1 was

Note: Supplementary data for this article are available at Cancer Research Online (http://cancerres.aacrjournals.org/).

Requests for reprints: Nancy Ratner, Division of Experimental Hematology, Cincinnati Children's Hospital Medical Center, 3333 Burnet Avenue, MLC 7013, Cincinnati, OH 45229. Phone: 513-636-9469; Fax: 513-636-3549; E-mail: Nancy.Ratner@cchmc.org.

doi:10.1158/0008-5472.CAN-05-3330

established according to published criteria (NIH Consensus Statement). Frozen, archived tumor specimen pathology was reviewed and RNA isolated and then analyzed on Affymetrix U95Av2 GeneChip microarrays as reported (18).

Cell culture. T265p21, 90-8, ST88-14, 88-3, and STS26T cell lines were provided by Jeff DeClue (National Cancer Institute, Bethesda, MD). The YST-1 cell line was provided by Yoji Nagashima (University School of Medicine, Yokohama, Japan). Human Narf cells that express isopropyl-L-thio-B-D-galactopyranoside (IPTG)–inducible human ADP ribosylation factor (ARF) were provided by Gordon Peters (Imperial Cancer Research Fund, London, United Kingdom). ST88-14, STS26T, S520, S462, and Narf lines were grown in DMEM (Fisher Scientific, Pittsburgh, PA) supplemented with 10% fetal bovine serum (FBS; Harlan, Indianapolis, IN). 88-3, 90-8, and T265p21 lines were grown in a RPMI 1640–based medium as described (7). The YST-1 line was grown in RPMI 1640 (Fisher Scientific) containing 10% FBS. NHSCs were generated as previously described (19). Analyses were done under standard culture conditions for each cell line. Several assays were not conducted on the 88-3 cells due to difficulties in culturing this line.

***NF1* mutation analysis.** DNA was isolated from frozen STS26T or YST1 cell pellets. The *NF1* gene was screened for mutations by denaturing high-performance liquid chromatography–based heteroduplex analysis using the WAVE analysis system (Transgenomic, Omaha, NE) as described. Several primer sequences were redesigned to reduce their homology to the *NF1* pseudogenes sequences (20).

3-(4,5-Dimethylthiazol-2-yl)-2,5-diphenyltetrazolium bromide assay. Cells (5×10^3) were plated in triplicate on a 24-well plate (day 0). The 3-(4,5-dimethylthiazol-2-yl)-2,5-diphenyltetrazolium bromide (MTT) assay was done on day 1 and day 4 by adding 50 μL of a 5 mg/mL MTT solution (Sigma-Aldrich, St. Louis, MO) to each well. Following incubation at 37°C for 2 hours, the formazan precipitate was extracted in isopropanol-HCl and absorbance measured at 540 nm. For Taxol sensitivity assays, the noted concentration of paclitaxel (Sigma-Aldrich) was added to the medium on day 1. Concentration of paclitaxel was based on previous studies (21).

Viability assay. Cells were cultured on glass coverslips. Live versus dead cell numbers were determined using a LIVE/DEAD Viability/Cytotoxicity kit (Molecular Probes, Eugene, OR) according to the protocol of the manufacturer. The total number of live and dead cells was counted in five fields per sample and averaged. Assays were done in duplicate.

Bromodeoxyuridine incorporation. Twenty-four hours post plating 3×10^4 cells onto glass coverslips, cells were labeled for 1 hour with bromodeoxyuridine (BrdUrd) labeling reagent (1:1,000; Amersham Biosciences, Piscataway, NJ) to detect DNA synthesis. Cells were fixed with 3.7% formaldehyde (Fisher Scientific), permeabilized in 0.3% Triton X-100 (Sigma-Aldrich), and incubated with anti-BrdUrd antibodies (1:200; Accurate Chemical & Scientific, Westbury, NY) in immunofluorescence buffer [20 mmol/L $MgCl_2$, 50 units DNase I (Roche, Basel, Switzerland)] for 45 minutes at 37°C. Cell nuclei and BrdUrd localization were visualized by incubating in 5 μg/mL bisbenzamide (Sigma-Aldrich) and rhodamine-conjugated donkey anti-Rat secondary antibodies (1:100; Jackson ImmunoResearch, West Grove, PA). Total number of cells and number of BrdUrd-positive cells were counted in five fields per sample and averaged. Assays were done in duplicate.

Western blot analysis. Cells were lysed on ice in 50 mmol/L Tris (pH 7.5), 120 mmol/L NaCl, 1 mmol/L EDTA, 0.5% NP40, 0.1 mmol/L sodium vanadate, 1 mmol/L sodium flouride, 5 μg/mL leupeptin, and 30 μmol/L phenylmethylsulfonyl flouride. Lysates were sonicated and clarified by centrifugation. Equivalent amounts of protein (50-100 μg) were separated by electrophoresis on SDS-polyacrylamide gradient gels (7-15% or 4-20%; ISC BioExpress, Kaysville, UT) and transferred to polyvinylidene difluoride membrane (Bio-Rad, Hercules, CA). Membranes were probed with anti-ARF (NB 200-111; Novus Biologicals, Littleton, CO), anti-RB (clone G3-245; BD Biosciences PharMingen, San Diego, CA), anti-p16 (Ab-1; Research Products, San Diego, CA), anti-p53 (D0-1; Santa Cruz Biotechnology, Santa Cruz, CA), anti-HDM2 (2A10 hybridoma supernatant provided by Gerry Zambetti, St. Jude Children's Research Hospital, Memphis, TN, and Arnold Levine, Cancer Institute of New Jersey/UMDNJ, New Brunswick, NJ), or anti-TWIST1 antibodies (22). Blots were stripped and reprobed with antitubulin (Sigma-Aldrich) or anti-β-actin (Cell Signaling Technology, Inc., Danvers, MA) as a loading control. Signals were detected using horseradish peroxidase–conjugated secondary antibodies (Bio-Rad, Hercules, CA) in combination with Enhanced Chemiluminescence (ECL) Plus developing system (Amersham Biosciences) according to the specifications of the manufacturer. For TWIST1 quantification, ImageJ 1.33u software (http://rsb.info.nih.gov/ij/) was used to obtain values from scanned autoradiographs representing protein levels. TWIST1 levels were normalized to β-actin levels for each sample.

Immunohistochemistry. Cell suspensions were mounted in a HistoGel (Richard Allan-Scientific, Kalamazoo, MI) "button" according to the protocol of the manufacturer and embedded in paraffin blocks. S100β and EGFR protein expression was determined by a semiautomated immunohistochemical technique as described (Ventana ES, Ventana Medical Systems, Tuscon, AZ; ref. 14).

RNA isolation and microarray hybridization. Total RNA was isolated from cells using Trizol reagent (Invitrogen, San Diego, CA) followed by phenol/chloroform extraction and ethanol precipitation. RNA integrity was verified with an Agilent Bioanalyzer 2100 (with typical 28S/18S ratios = 2 ± 0.1). To generate a biotinylated probe, cDNA was synthesized (Superscript cDNA synthesis kit, Invitrogen, San Diego, CA) from 10 μg RNA using an oligo(dT) primer with a T7 RNA polymerase promoter at the 5′ end. The cDNA was made double stranded and used in an *in vitro* transcription reaction (Enzo Diagnostics) with T7 RNA polymerase to synthesize biotinylated product for hybridization to Affymetrix GeneChips HU133A and HU133B using the Affymetrix recommended protocol. The Affymetrix Gene Array scanner and Micro Array Suite version 5.0 were used to scan and quantify GeneChips using default settings.

Microarray data analysis. Microarray gene expression data (MAS *.cel files) were initially processed using Robust Microarray Analysis (RMA; ref. 23). RMA data were loaded into Genespring 6.1 computer software (Silicon Genetics, Redwood City, CA), transformed from a log 2 to linear scale, and normalized per gene to the mean value of its level of expression across seven NHSC samples. Welch *t* test/ANOVA with Benjamini multiple testing correction was used to identify statistically significant differences in gene expression between groups. Unsupervised hierarchical cluster analysis using Pearson correlation for a distance metric was used to arrange genes according to similar expression patterns. Statistical analysis of functional classification was used to identify altered molecular pathways (OntoExpress; http://vortex.cs.wayne.edu/ontoexpress/). For analysis of primary MPNSTs, raw data (*.cel) were RMA-processed, assigned a U133 identification number, and imported into GeneSpring 6.1 for further analysis. To compare the primary MPNST data to the MPNST cell line and NHSC data, an additional per chip normalization to the median was conducted, followed by per gene normalization to the NHSC samples. To identify TWIST1 binding sites (24) in putative gene promoter regions, the pattern search program from GEMS Launcher (http://www.genomatix.de) was used to scan sequences with the IUPAC pattern.

Quantitative real-time reverse transcription-PCR. Total RNA was used as a template to synthesize double-stranded cDNA using an oligo(dT) primer with Superscript II reverse transcriptase (Invitrogen). Duplicate reactions omitting reverse transcriptase were conducted to control for genomic DNA contamination. Relative levels of RNA were measured by quantitative real-time PCR using the ABI 7500 Sequence Detection System default settings. For most genes, amplification was conducted in SYBR Green Master Mix (Applied Biosystems, Foster City, CA). See Supplementary Table S1 for primer sequences for individual genes. Cycle threshold values were obtained where fluorescence intensity was in the geometric phase of amplification and averaged for triplicate reactions. Values for individual genes of interest were normalized to values for *β-actin* and used to calculate fold change in gene expression using ABI software. *SOX10* (ABI TaqMan Probe ID Hs00366918_m1) and 18S (ABI TaqMan Probe ID Hs99999901_s1) were amplified using ABI 2X Universal TaqMan Master Mix (Applied Biosystems).

Small interfering RNA transfection. MPNST cells were plated in DMEM containing 10% FBS and no antibiotic for transfection the following day. Small interfering RNA (siRNA) molecules (si*TWIST1* SMARTpool or si*CONTROL* Non-Targeting siRNA Pool; Dharmacon, Lafayette, CO) were

diluted in serum-free DMEM and incubated with XtremeGENE siRNA transfection reagent (Roche) at room temperature for 20 minutes before dropping on cells at a final optimal concentration of 20 nmol/L. Cell medium was changed 24 hours posttransfection to minimize toxicity. Cells were incubated 1 to 5 days before analyses. Transfection efficiency was ~90% as determined with a fluorescent siGLO control (Dharmacon).

Migration assay. The migratory response of MPNST cells was measured using a modified Boyden chamber assay. Four days posttransfection with siRNA (Dharmacon):XtremeGENE (Roche) complexes or XtremeGENE reagent alone, 4×10^4 cells in serum-free DMEM were plated on the upper chamber of a transwell with 8-μm pores (Costar, Corning Inc., Corning, NY). The lower chamber contained 800 μL MPNST conditioned medium. Cells were incubated for 16 hours at 37°C in 10% CO_2. Nonmigrating cells were removed from the upper surface of the membrane with cotton swabs. Membranes were stained with bisbenzimide and mounted onto glass slides. Migration was quantified by counting cells in four fields. Each condition was done in triplicate and the number of migrated cells was normalized to the total number of cells on an unscraped filter to validate the total number of cells plated. Data shown are representative of three independent experiments; values presented are the mean ± SD. Statistical significance was determined by *t* test using Microsoft Excel software.

Results

A collection of MPNST cell lines. Eight MPNST cell lines were collected for analysis (Table 1). Six cell lines were derived from NF1 patients. Two cell lines were derived from sporadic MPNSTs. NHSCs were chosen as a control because Schwann cells or their precursors are the most likely cells of origin in MPNSTs. Patient information and histopathology of the primary tumors have previously been documented in the original articles cited in Table 1.

We confirmed that the sporadic MPNST lines STS26T and YST-1 were wild-type at the *NF1* locus. All 60 exons of the *NF1* gene were screened for mutations using denaturing high-performance liquid chromatography–based heteroduplex analysis. No mutations were detected in the coding region of the *NF1* gene in either sporadic MPNST sample (data not shown). Loss of heterozygosity (LOH) at the *NF1* locus has previously been confirmed in five of the six NF1-associated MPNST lines (8, 25, 26).

Cell growth rate varies in MPNST cell lines. We compared growth properties of the MPNST cell lines by cell accumulation assays (Fig. 1). There was no correlation with NF1 status and growth rate. The fastest growing cell lines were STS26T, a sporadic MPNST line, and T265p21, an MPNST line derived from an NF1 patient (Fig. 1*A*). The more slowly proliferating cell lines, S520, 90-8, and YST-1, evidenced density-dependent growth. At higher plating densities, they showed more robust growth but the overall trend in relative rates of cell accumulation remained the same (data not shown). We determined whether different rates of cell cycle progression or cell death accounted for the large variation in cell proliferation among the MPNST cell lines. BrdUrd labeling of the MPNST cell lines showed that their rates of BrdUrd incorporation paralleled their relative rates of proliferation (Fig. 1*B*). In contrast, the rates of cell death were approximately constant in all of the lines (Fig. 1*C*). Thus, rates of cell proliferation vary among the MPNST cell lines and do not distinguish the NF1-associated MPNSTs from the sporadic MPNSTs.

Cell cycle proteins and Schwann cell markers are altered in MPNST cell lines. Functional disruptions of the pRb tumor suppressor pathway are frequent events in primary MPNSTs

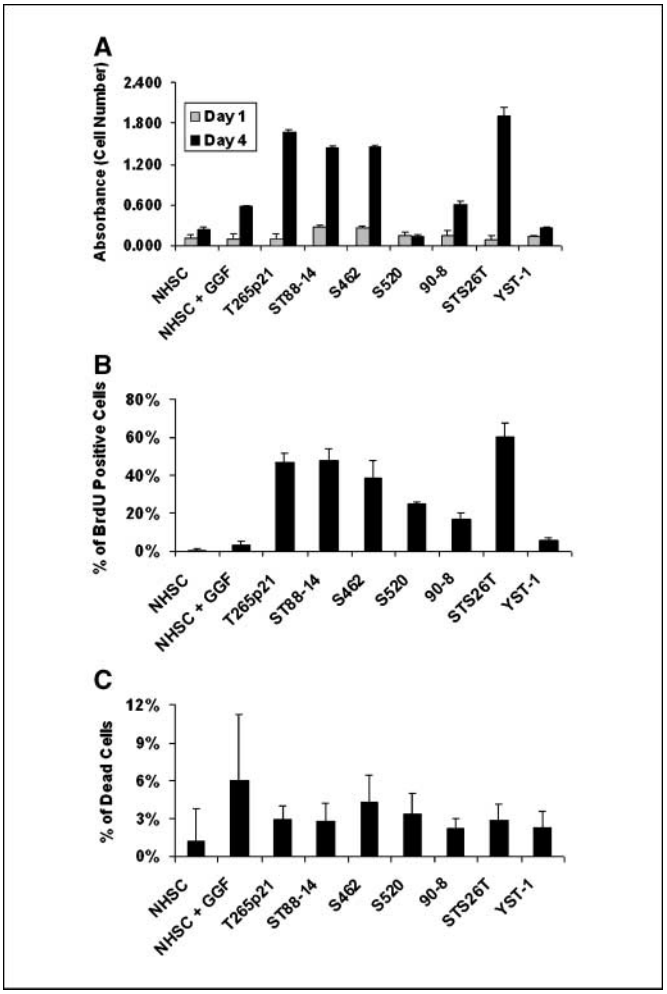

Figure 1. Cell growth rates vary in MPNST cell lines. MPNST cells were seeded at equivalent cell numbers in their normal growth medium. The same number of NHSCs was plated in the absence (*NHSC*) or presence of glial growth factor (*NHSC + GGF*). *A,* 5×10^3 cells were plated in triplicate on day 0. MTT assays were done on day 1 and day 4. Absorbances were normalized to a medium-only control. *B,* 3×10^4 cells were plated. Twenty-four hours later, cells were labeled with BrdUrd for 1 hour and then stained for BrdUrd incorporation. Percent of cells staining positively for BrdUrd incorporation. At least 300 cells were counted per cell type on duplicate coverslips. *C,* 3×10^4 cells were plated. Twenty-four hours later, cells were stained with Calcein-AM and ethidium homodimer-1. Percent of cells staining positively for ethidium-1. Approximately 400 cells were counted per cell type on duplicate coverslips. *Columns,* mean of two independent experiments; *bars,* SD.

Table 1. MPNST cell lines

Cell line	NF1 Patient	Reference
ST88-14	+ (LOH)	(7)
90-8	+ (LOH)*	(8)
88-3	+ (LOH)	(8)
T265p21	+	(9)
S462	+ (LOH)	(10)
S520	+ (LOH)	(10)
STS26T	−	(11)
YST-1	−	(12)

NOTE: +, documented history of NF1 disease; −, no documented history of NF1 disease.
*Cell line with a known microdeletion of *NF1* (26).

(17, 27–29) due to inappropriate pRb phosphorylation via dysregulation of upstream regulators (*p16^{INK4a}* mutation or cyclin overexpression) or loss of the pRB gene itself. pRb immunoreactivity was detected in all of the MPNST lines, suggesting that the *RB* gene itself is not lost in the tumor cells (Fig. 2*A*). In comparison with NHSCs, an increase in the inactive or phosphorylated form of pRb was detected in the 90-8, S520, ST88-14, STS26T, and YST-1 cell lines. Overexpression of cyclin-dependent kinase 4 (CDK4) or loss of the p16^{INK4a} tumor suppressor can both result in enhanced pRb phosphorylation. CDK4 was not differentially expressed between the MPNST cell lines and NHSCs (data not shown). In contrast, p16^{INK4a} was expressed only in cells that were wild-type for neurofibromin, NHSCs, and the two sporadic MPNST lines (Fig. 2*A*). These results suggest that p16^{INK4a} is selectively inactivated in the NF1-associated MPNST cell lines.

The *p53* tumor suppressor gene is frequently deleted, mutated, and/or overexpressed in primary MPNSTs (15–17, 28). Therefore, we assessed the integrity of the p14^{ARF}-HDM2-p53 signaling pathway in the MPNST cell lines in comparison with NHSCs. p14^{ARF} was only expressed in the sporadic MPNST cell line STS26T (Fig. 2*A*). In addition, all MPNST cell lines showed a significant increase in HDM2 expression, a negative regulator of p53, in comparison with NHSCs (Fig. 2*B*). Notably, p53 was highly overexpressed in two of the MPNST cell lines, S520 and S462, whereas a lower molecular weight species (likely a truncated form of p53) was overexpressed in the 90-8 line in comparison with NHSCs (Fig. 2*B*). The remaining MPNST lines, ST88-14 and T265p21, both showed levels of p53 expression that were modestly higher than that in NHSCs. One sporadic MPNST line, YST-1, also exhibited a slight overexpression of p53 in comparison with NHSCs whereas p53 expression was completely absent in the STS26T sporadic MPNST line.

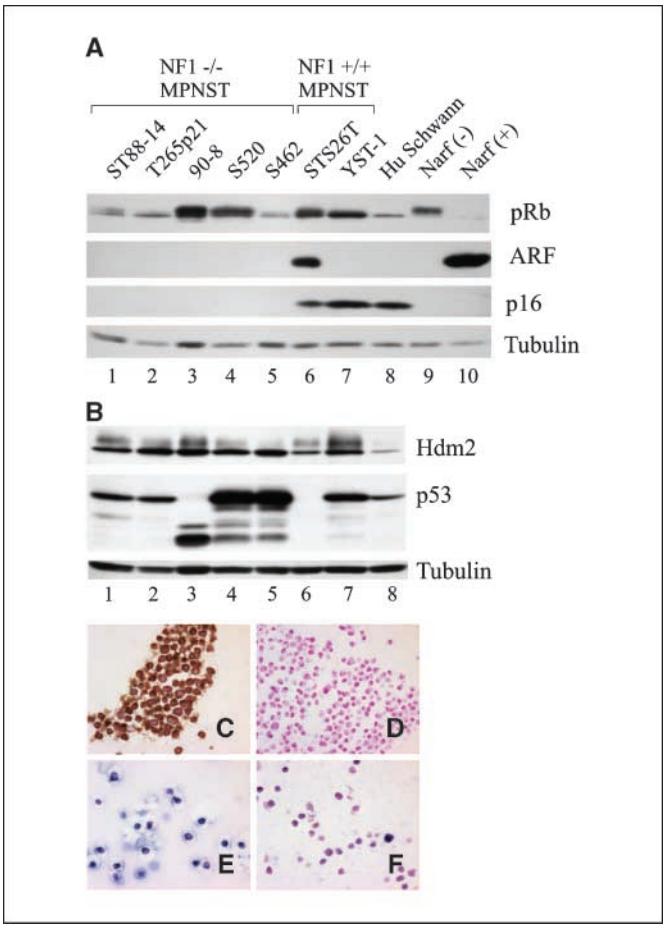

Figure 2. Cell cycle proteins are altered in MPNST cell lines. *A* and *B,* equal amounts (100 μg/lane) of NF1-associated MPNST cell lysates (*NF1$^{-/-}$ MPNST*), sporadic MPNST cell lysates (*NF1$^{+/+}$ MPNST*), and NHSC (*Hu Schwann*) lysates were immunoblotted with the antibodies indicated. Blots were stripped and reprobed for tubulin as a loading control. Human Narf cells that express IPTG-inducible human ARF were used as a control for ARF expression and for pRb hypophosphorylation in the growth-arrested, IPTG-treated (+) cells. ARF was induced by treatment of cells with (+) or without (−) 1 mmol/L IPTG for 48 hours. Positive staining is brown for S100β and blue for EGFR in (*C-E*). *C,* immunohistochemical staining of NHSCs for S100β protein and EGFR. *D,* corresponding sample of NHSCs that omitted incubation with primary antibodies. *E,* immunohistochemical staining of the NF1-associated cell line ST88-14 for S100β protein and EGFR. Representative of all of the MPNST cell lines except YST-1. *F,* immunohistochemical staining of the sporadic MPNST cell line, YST-1, for S100β protein and EGFR.

De novo EGFR expression has previously been implicated as an early event in Schwann cell transformation (14, 30). We stained NHSCs and the MPNST cell lines for EGFR and double labeled with the Schwann cell marker S100β protein. NHSCs are S100β positive and EGFR negative (Fig. 2*C*). All of the NF1-associated MPNST lines and one sporadic MPNST line, STS26T, were strongly immunoreactive for EGFR in 100% of the cells (Fig. 2*E*). The sporadic MPNST line YST-1 exhibited moderate EGFR expression in ~50% to 60% of the cells (Fig. 2*F*). All of the MPNST cell lines currently lack S100β protein expression (Fig. 2*E* and *F*) although S100β immunoreactivity was originally reported for ST88-14, T265p21, and YST-1 (9, 12, 31). Thus, MPNST lines aberrantly express EGFR and lack expression of a Schwann cell marker, perhaps reflecting progressive anaplasia or loss of differentiation.

Gene expression profile of MPNST cell lines is consistent in MPNST *in vivo*. To identify gene expression changes associated with malignant transformation of Schwann cells, we did global gene expression analysis of MPNST cell lines using microarray technology. We analyzed samples from six NF1-associated MPNST lines, two sporadic MPNST cell lines, and seven NHSC samples on Affymetrix GeneChips containing >45,000 probe sets (~39,000 transcripts and ~33,000 annotated genes). To identify genes consistently expressed within the MPNST cell lines and relevant to Schwann cells, we compared average MPNST cell line gene expression to average NHSC gene expression and identified 941 probe sets differentially expressed by ≥3-fold, 841 of which were statistically significant ($P < 0.01$, Welch *t* test with Benjamini correction). To minimize false positives, we eliminated genes differentially expressed 3-fold in at least one normal reference sample (NHSC), reducing the number of probe sets to 592 consistently expressed among NHSCs and differentially expressed in MPNST cell lines (Fig. 3*A*).

Statistical analysis of functional classifications of these genes emphasized cell growth and differentiation, cell adhesion/migration, and immune response as key dysregulated cellular systems. Decreased expression of many Schwann cell markers, including *S100B, PMP-22, NGFR, CNP*, and *SOX10*, indicates aberrant differentiation in the MPNST cells. However, *GFAP* and *MBP* are expressed at similar levels in NHSC and the MPNST cell lines. Alterations in the pRb and p53 pathways are supported by the up-regulation of nine E2F targets (32) and three p53 targets, *GADD-45* (33), *Sema3B* (34), and *DDA3* (35). Genes within the MPNST molecular profile do not overlap with a generalized tumor cell line list generated by microarray analysis of the NCI 60 cancer lines (36) or a list of 24 genes up-regulated in synovial sarcomas and 4 MPNSTs (37).

To validate the data and to assess the utility of MPNST cell lines as a model for MPNST *in vivo*, the microarray data generated from the MPNST cell lines and NHSC were compared with microarray

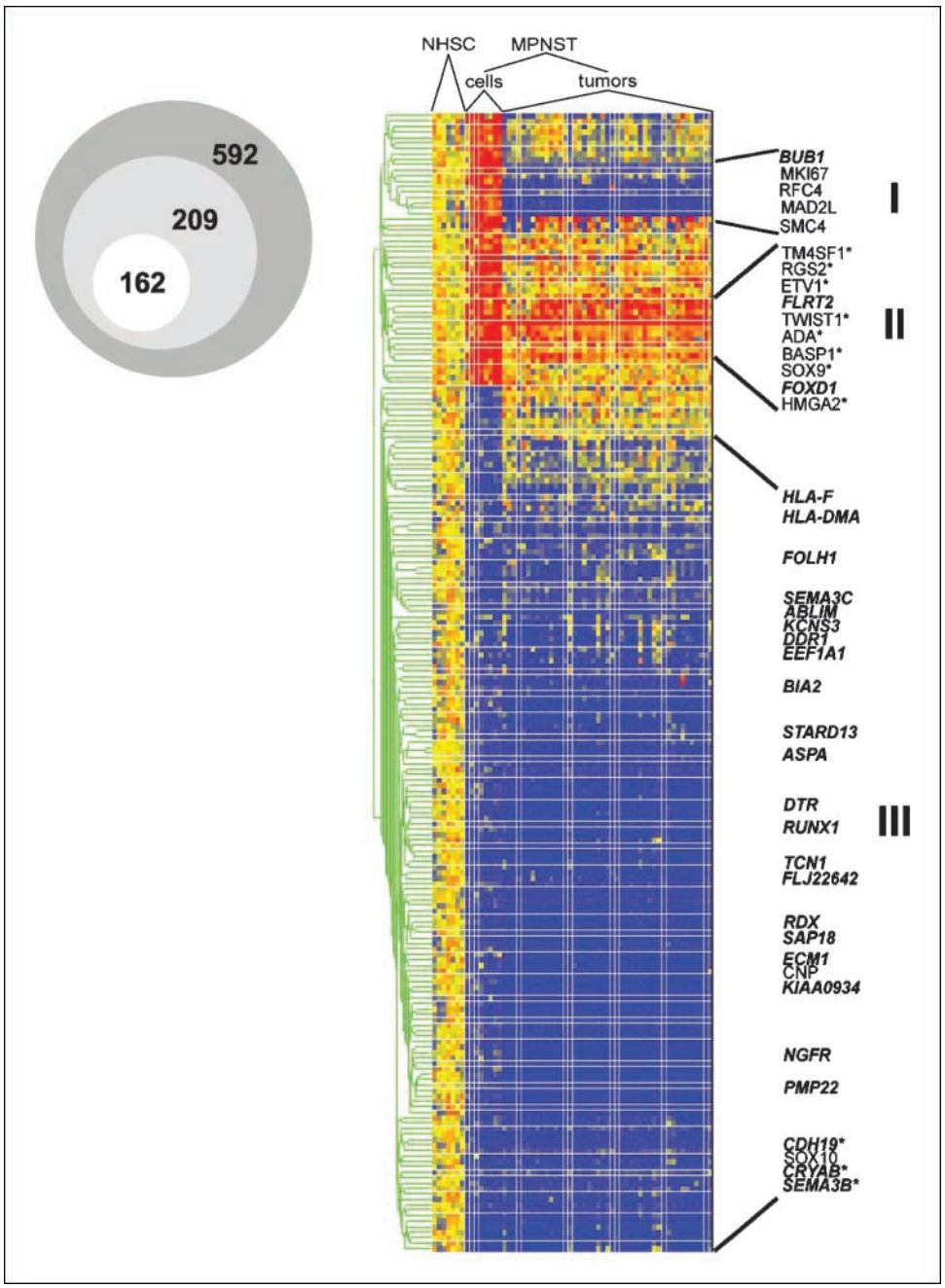

Figure 3. Microarray gene expression profile of MPNST cell lines and primary MPNST. RNA samples from seven NHSC, two sporadic MPNST cell lines, and six NF1-associated cell lines were labeled and hybridized to Affymetrix U133 GeneChips. Gene expression data were analyzed with Genespring 6.1. Gene expression was normalized to NHSC (*yellow*); overexpression (*red*); underexpression (*blue*). *A,* schematic of filtering process to obtain genes representing the MPNST molecular signature. 592 probe sets represented genes differentially expressed 3-fold in MPNST cell lines compared with NHSC ($P < 0.01$, with Benjamini multiple testing correction). 209 of 592 probe sets were represented in primary MPNST data set (Affymetrix U95). 162 of 209 probe sets were consistently expressed among MPNST cell lines and primary MPNSTs. *B,* expression profile of 209 probe sets differentially expressed in MPNST cell lines and represented in the microarray data from 45 primary MPNSTs. Cluster analysis reveals three distinct clusters: *I,* genes up-regulated in MPNST cell lines but down-regulated in primary MPNSTs (*SMC4L1, MAD2L1, RFC4, MKI67, BUB1*) promote cell cycle progression; *II,* genes up-regulated in all MPNSTs (putative oncogenes *TM4SF1, RGS2, ETV1, TWIST1, ADA, BASP1, SOX9, HMGA2*); *III,* genes down-regulated in all MPNSTs (Schwann cell markers *SOX10, CNP, NGFR, PMP22*). See Supplementary Table S2 for complete list. *, genes previously reported as aberrantly expressed in other tumor systems, putative oncogenes, or tumor suppressor genes. Bold italicized genes contain the TWIST1-specific E-box (24) in their upstream sequence, potential transcriptional targets of TWIST1.

data generated from 45 primary MPNST samples hybridized to Affymetrix U95 chips, containing ~12,000 probe sets representing ~10,000 annotated genes (18). Nearly all of the genes represented on the U95 chip were also on the U133 chip, resulting in 9,433 overlapping genes. Unsupervised hierarchical cluster analysis of the 9,433 probe sets across all samples distinguished normal samples, NHSCs, from tumor samples, MPNST cells, and primary MPNSTs (data not shown). When we examined expression of the 592 probe sets differentially expressed in MPNST cell lines (described above) in the primary MPNST samples, approximately one third (209 of 592) were represented on both the U133 and U95 chips (Fig. 3*A*). Therefore, the gene list we refer to as the MPNST molecular signature is not a complete profile of global gene expression. However, the majority (162 of 209) of probe sets that distinguished MPNST cells from NHSCs and were represented on both platforms predicted gene expression changes in solid tumors, validating the use of the MPNST cell lines as an *in vitro* tumor model system. Three genes were represented by duplicate probes, resulting in a 159-gene signature for MPNST.

Hierarchical cluster analysis of the 209 probe sets differentially expressed in MPNST cell lines and represented in the primary MPNST data set revealed three distinct clusters (see Supplementary Table S2): (*a*) 10 genes up-regulated in MPNST cell lines but down-regulated in primary MPNSTs, (*b*) 13 genes up-regulated in all MPNST samples, and (*c*) 146 genes down-regulated in all MPNST samples (Fig. 3*B*). The 10 genes in cluster I are differentially expressed compared with NHSC but the levels of expression are not consistent between the MPNST cell lines and the primary MPNST

samples. The protein products of most of these genes are involved in cell cycle progression. It is reasonable to believe that cell lines growing in tissue culture medium may be exposed to nonphysiologic growth-promoting conditions *in vitro*. Many genes in cluster II have been implicated in other tumor systems. Genes in cluster III include Schwann cell differentiation markers, validating the notion that MPNST cells do not exhibit properties of differentiated Schwann cells.

TWIST1 overexpression is necessary for MPNST cell migration but not apoptosis or chemoresistance. *TWIST1* gene expression was up-regulated in all MPNST cell lines and all primary MPNSTs as compared with normal Schwann cells. Differential expression of *TWIST1* was confirmed at the RNA level by quantitative real-time reverse transcription-PCR (Fig. 4*A*) and at the protein level by Western blotting (Fig. 4*B*). To study the functional significance of TWIST1 overexpression in MPNST cells, we inhibited TWIST1 expression using siRNA molecules. We reduced TWIST1 expression at both the RNA and protein levels to ~10% to 20% compared with cells transfected with a nontargeting siRNA control (Fig. 4*C*). Putative TWIST1 transcriptional targets (n = 27) were identified by promoter analysis. Differential expression of 8 of 10 targets was validated by quantitative real-time PCR but the expression of none was altered by siRNA exposure for 5 days (data not shown). Furthermore, expression of known TWIST1 targets (38–40) was not significantly different in MPNST samples as compared with NHSCs.

TWIST1 can cause tumor cell resistance to microtubule-stabilizing drugs such as Taxol (21), an interesting finding given the relative chemoresistance of MPNSTs. We ascertained Taxol resistance of MPNST cell lines. All of the MPNST cell lines follow the survival curve of the TWIST1-expressing positive control cell line, PC3, indicating that they are relatively resistant to Taxol-induced cell death (Fig. 5*A*). IC_{50} values for individual MPNST cell lines were statistically different from the LNCaP TWIST1 negative control (P < 0.001; data not shown). However, reducing TWIST1 expression in MPNST cells by transient transfection with TWIST1 siRNA did not affect chemosensitivity (Fig. 5*B*). TWIST1 has also been shown to inhibit apoptosis (38). Neither cell growth nor apoptosis was altered in MPNST cells transfected with TWIST1 siRNA (data not shown).

TWIST1 can promote tumor cell migration, invasion (41), and metastasis (39). To examine TWIST1 function in MPNST migration, we tested whether MPNST cells were migratory in an *in vitro* migration assay. Interestingly, the MPNST cells did not have a haptotactic phenotype; they did not migrate in the serum-free or serum-containing medium. Because EGFR is overexpressed in MPNST cells, we added EGF to the standard serum-containing medium but observed minimal migration. MPNST conditioned medium was required for significant chemotactic migration (data not shown), suggesting that MPNST cells may be secreting as yet unidentified chemoattractant(s). Migration was inhibited by 75% in STS26T MPNST cells transfected with TWIST1 siRNA (Fig. 5*C*). Thus, MPNST cell migration is dependent on TWIST1 expression itself or expression of TWIST1 transcriptional targets.

Discussion

We compared primary human Schwann cells to 8 MPNST cell lines and 45 solid MPNSTs. Rates of proliferation and gene expression profiles of the MPNST cell lines were variable, mirroring the heterogeneity of these tumors *in vivo*. Nevertheless, our microarray gene expression analyses of Schwann cells and MPNST lines resulted in the identification of a specific 159-gene profile for MPNST that was validated in a large panel of primary MPNSTs. The genes in the MPNST signature, many of which have been implicated in other types of cancer, represent potential regulators of MPNST pathogenesis.

Disruption of cell cycle regulation was apparent in the MPNST cell lines but consistent alterations in neither pRb-related nor p53-related proteins were observed. The $p16^{INK4a}$ protein was absent in five of five NF1-associated MPNST cell lines whereas both sporadic lines and NHSCs retained $p16^{INK4a}$ expression. Homozygous deletion of $p16^{INK4a}$ has been detected in both NF1-associated and sporadic MPNSTs, but not in benign neurofibromas, suggesting that its loss contributes to malignant transformation

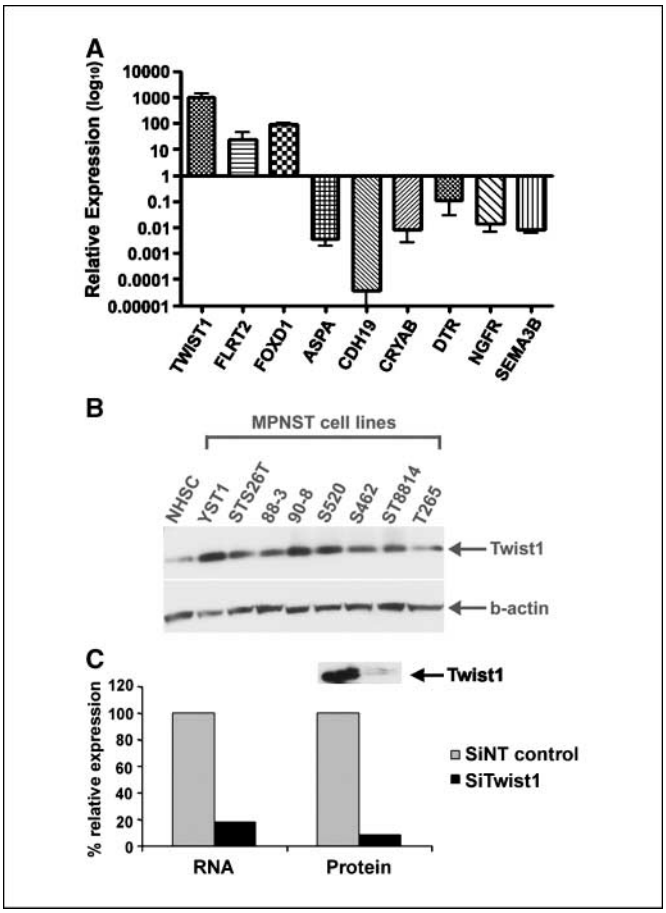

Figure 4. TWIST1 and potential TWIST1 targets are differentially expressed in MPNST compared with NHSC. *A,* confirmation of differential expression of *TWIST1* and potential transcriptional targets of TWIST1 in MPNST cell lines compared with NHSC by quantitative real-time PCR. *Columns,* average expression value for MPNSTs relative to NHSC set at 1 (log_{10} scale); *bars,* SD. Differential expression in the same direction was confirmed for 8 of 10 potential TWIST1 transcriptional targets in all MPNST cell lines; ECM1 and SAP18 differential expression was confirmed in some, but not all, MPNST cell lines (data not shown). *B,* confirmation of differential expression of TWIST1 protein by Western blotting. The protein blot was probed first with anti-TWIST1 antibodies, stripped, and reprobed with antiactin antibodies as a loading control. ImageJ 1.33u software was used to quantify ECL signal representing amount of protein. TWIST1 levels were normalized to β-actin levels for each sample. TWIST1 levels were 2- to 10-fold higher in MPNSTs compared with NHSC. *C, TWIST1* siRNA reduces expression of *TWIST1* RNA and TWIST1 protein. STS26T MPNST cells were transfected with TWIST1 siRNA or a nontargeting control siRNA (*SiNT*) and assayed for TWIST1 expression 2 to 5 days posttransfection. Data are shown for day 5. *Columns,* levels of expression relative to the nontargeting control siRNA for either RNA or protein. RNA levels were measured using quantitative real-time PCR; protein levels were quantified using ImageJ software. *Arrow,* band detected by TWIST1 antibodies on a Western blot.

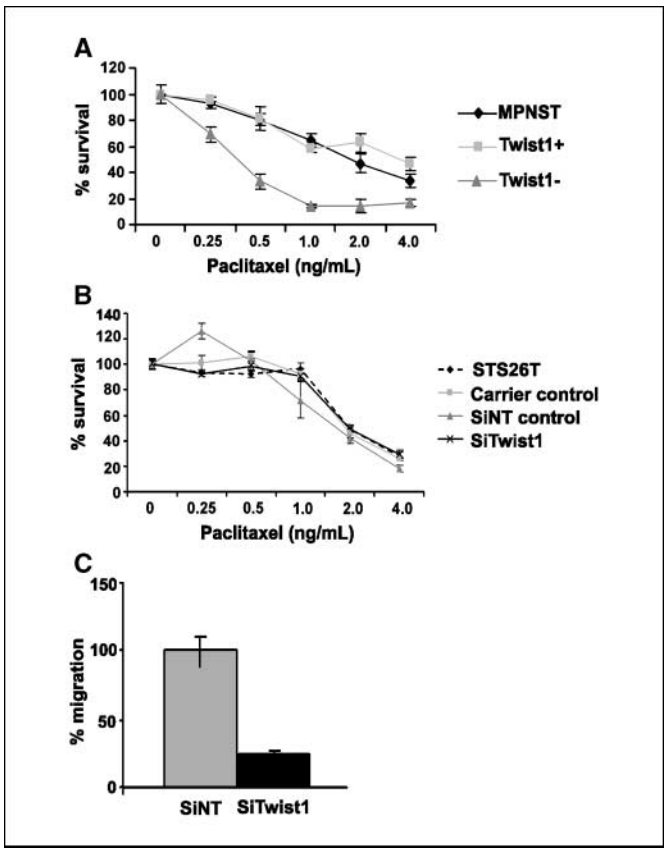

Figure 5. Reducing TWIST1 expression does not affect MPNST chemoresistance but inhibits cell chemotaxis. *A,* MTT assay measuring MPNST cell accumulation in the presence of 0, 0.25, 0.5, 1.0, 2.0, or 4.0 ng/mL paclitaxel for 3 days. Cell survival is presented as percent of survival in DMSO carrier control. Each dose was conducted in triplicate. *Points,* mean of at least three independent experiments and for all MPNST cell lines; *bars,* SE. *PC3 (pos),* TWIST1 positive control; *LNCaP (neg),* TWIST1 negative control (21). *B,* MTT assay measuring STS26T MPNST cell accumulation as in (*A*) 4 days posttransfection with TWIST1 siRNA or a nontargeting control siRNA. *C,* migration assay of STS26T MPNST cells 4 days posttransfection with TWIST1 siRNA or a nontargeting control siRNA. *Points,* percentage of cells migrating through a transwell filter relative to the nontargeting control siRNA; *bars,* SE. The number of migrating cells is significantly less in cells transfected with siTWIST1 ($P < 0.001$). Representative of three independent experiments.

(27, 30, 42). Although loss of $p16^{INK4a}$ would be predicted to enhance pRb phosphorylation, we found no clear correlation between the expression level or phosphorylation status of pRb and the presence of $p16^{INK4a}$ in the MPNST cells. Comparative analysis of ARF revealed a lack of expression in all cells examined except the sporadic MPNST line STS26T. Detection of ARF in STS26T is consistent with the absence of p53 in those cells. The absence of ARF in primary NHSCs is not surprising because ARF is repressed by a variety of factors in normal cells. Others have shown that dual loss of $p16^{INK4a}$ and ARF pathways is required for transformation by Ras, EGFR, and other oncogenes (reviewed in ref. 43).

The microarray data confirmed differential expression of some genes that have previously been implicated in NF1 tumor formation but solely in subsets of cell lines and tumors. Midkine is a secreted protein that promotes angiogenesis and is up-regulated in a variety of tumors (reviewed in ref. 44), including 5 of 8 of the MPNST cell lines and 22 of 45 of the primary MPNST samples. We observed *CD44* overexpression in 3 of 8 MPNST cell lines but no primary MPNSTs (45). Whereas HGF/c-Met signaling can promote MPNST invasion, there was no indication of dysregulated c-Met-related genes in our MPNST microarray data; secretion of HGF and signaling through c-Met may not be apparent at the transcriptional level (46). We confirmed that all MPNST cell lines, but not NHSCs, were positive for EGFR protein. Our previous analysis of the MPNST primary tumors revealed a statistically significant difference in expression profiles of EGFR-positive versus EGFR-negative MPNSTs (18). These observations suggest that aberrant expression of these genes may not be necessary for Schwann cell transformation and/or MPNSTs expressing these genes may represent a distinct subclass. Alternatively, these genes may be expressed in different populations of cells within each primary tumor.

Genes that are down-regulated in the MPNST molecular profile include several markers of Schwann cell differentiation, suggesting that MPNST cells have dedifferentiated or represent a Schwann cell precursor that has acquired mutations leading to tumor formation. *SOX10* expression is down-regulated in MPNSTs and normally regulates expression of genes promoting Schwann cell differentiation (47). A recent study by Levy et al. (48) reports reduced levels of *SOX10* and other Schwann cell markers in 9 MPNST samples compared with 14 benign neurofibroma samples by quantitative real-time PCR. SOX9 (49) and TWIST1 (24) are expressed in neural crest stem cells, Schwann cell precursors, and are overexpressed in MPNSTs compared with NHSCs. Although Schwann cells are the proposed cell of origin in MPNSTs, comparisons to additional tumors and normal tissues may reveal other genes relevant to MPNST formation or progression. The idea that tumor cells resemble progenitor cells is supported in other tumor models (50).

We identified *TWIST1* as a previously unrecognized cancer-related gene in MPNST. *TWIST1* gene expression is up-regulated in both MPNST cell lines and primary tumors. TWIST1 is also overexpressed in other tumors, including sarcomas (21, 38, 39). TWIST1 is normally expressed early in development and regulates cell type determination and differentiation of mesodermal tissues (reviewed in ref. 24). TWIST1 inhibits expression of ARF, as observed in seven of eight of the MPNST cell lines, which results in a bypass of p53-induced apoptosis (38). TWIST1 can inhibit apoptosis and promote cell transformation (38). However, we did not detect a significant change in apoptosis on reducing TWIST1 expression in MPNST cells. In several human carcinoma cell lines, TWIST1 can prevent cell death in the presence of microtubule-stabilizing chemotherapeutic agents (21) and stable suppression of TWIST1 increases sensitiviy to Taxol-induced cell death (41). MPNSTs are poorly responsive to standard chemotherapeutic regimens and we showed that MPNST cell lines are resistant to Taxol. However, transiently reducing TWIST1 expression did not result in Taxol sensitivity in our MPNST cell accumulation assay.

TWIST1 is necessary and sufficient for prostate cancer cell migration and invasion *in vitro* (41). Suppression of TWIST1 inhibits metastasis in a murine breast tumor model (39). MPNSTs are highly invasive tumors that commonly metastasize. Reducing TWIST1 expression in MPNST cells inhibited chemotaxis, a key component of the metastatic process. Although many of the genes that are overexpressed in MPNST cells compared with NHSCs are implicated in cell adhesion, migration, or invasion, none are known chemoattractants. It is possible that hypersecretion and not transcriptional overexpression of a chemoattractant may promote MPNST cell migration.

We conclude that whereas MPNST cell lines are heterogeneous in cellular growth, a common gene expression profile in MPNST cell lines and primary MPNSTs distinguishes them from normal Schwann cells. The MPNST cell lines thus provide a valuable

resource for generating *in vitro* evidence to support preclinical and clinical trials. Overexpression of TWIST1 is constant across all tested MPNST cell lines and primary tumors and is necessary for cell migration. Further investigation into the functional roles of TWIST1 and its transcriptional targets may help to uncover novel biomarkers or drug targets for improved diagnosis and treatment of MPNST.

Acknowledgments

Received 10/12/2005; revised 11/22/2005; accepted 1/5/2006.

Grant support: NIH grant NS28840 and DOD grants DAMD-17-01-0704 and W81XWH-04-1-0273 (N. Ratner); National Neurofibromatosis Foundation Young Investigator Award and NINDS Translational Neuroscience Award K01-NS049191-01A1 (S.J. Miller); Deutsche Krebshilfe grant 70-2635, 70-2794 (V. Mautner) and NCI U01 CA 84291 (B.J. Aronow).

The costs of publication of this article were defrayed in part by the payment of page charges. This article must therefore be hereby marked *advertisement* in accordance with 18 U.S.C. Section 1734 solely to indicate this fact.

We thank Dr. Erik Knudsen (University of Cincinnati) for helpful discussions; Yoji Nagashima and Jeff DeClue for providing MPNST cell lines; Jennifer O'Malley for generating quantitative real-time PCR data; Sian Griffiths and Claudia Consoli for technical assistance with *NF1* mutation analysis; the University of Miami organ procurement team (Les Olson, director) for procurement of normal human nerves; Dr. Patrick Wood of the Miami Project to Cure Paralysis; the Laboratory of Immunohistochemistry and Medical Pathology at the University of Cincinnati Medical Center (Dr. Sue Heffelfinger, Director) for the S100 β and EGFR immunohistochemistry; Cincinnati Children's Hospital Affymetrix gene chip core (Dr. Steve Potter and Shawn Smith) for microarray hybridization; and Dr. Carlotta Glackin (Beckman Research Institute of the City of Hope, Duarte, CA) for providing anti-TWIST1 antibody. We thank all the investigators who contributed MPNST cases including Tarik Tihan (University of California, San Francisco/formerly Johns Hopkins), Richard Prayson (Cleveland Clinic), Abjit Guha (University of Toronto), Julia Bridge (University of Nebraska) and Rosalie Ferner (King's College, London).

References

1. Helman LJ, Meltzer P. Mechanisms of sarcoma development. Nat Rev Cancer 2003;3:685–94.
2. Huson SM, Compston DA, Clark P, Harper PS. A genetic study of von Recklinghausen neurofibromatosis in south east Wales. I. Prevalence, fitness, mutation rate, and effect of parental transmission on severity. J Med Genet 1989;26:704–11.
3. Friedman JM, Gutmann DH, MacCollin M, Riccardi VM. Neurofibromatosis: phenotype, natural history, and pathogenesis. 3rd ed. Baltimore (MD): Johns Hopkins University Press; 1999.
4. Huson SM, Harper PS, Compston DA. Von Recklinghausen neurofibromatosis. A clinical and population study in south-east Wales. Brain 1988;111:1355–81.
5. Ferner RE, Gutmann DH. International consensus statement on malignant peripheral nerve sheath tumors in neurofibromatosis. Cancer Res 2002;62:1573–7.
6. Takeuchi A, Ushigome S. Diverse differentiation in malignant peripheral nerve sheath tumours associated with neurofibromatosis-1: an immunohistochemical and ultrastructural study. Histopathology 2001;39:298–309.
7. Fletcher JA, Kozakewich HP, Hoffer FA, et al. Diagnostic relevance of clonal cytogenetic aberrations in malignant soft-tissue tumors. N Engl J Med 1991;324:436–42.
8. Glover TW, Stein CK, Legius E, Andersen LB, Brereton A, Johnson S. Molecular and cytogenetic analysis of tumors in von Recklinghausen neurofibromatosis. Genes Chromosomes Cancer 1991;3:62–70.
9. Badache A, De Vries GH. Neurofibrosarcoma-derived Schwann cells overexpress platelet-derived growth factor (PDGF) receptors and are induced to proliferate by PDGF BB. J Cell Physiol 1998;177:334–42.
10. Frahm S, Mautner VF, Brems H, et al. Genetic and phenotypic characterization of tumor cells derived from malignant peripheral nerve sheath tumors of neurofibromatosis type 1 patients. Neurobiol Dis 2004;16:85–91.
11. Dahlberg WK, Little JB, Fletcher JA, Suit HD, Okunieff P. Radiosensitivity *in vitro* of human soft tissue sarcoma cell lines and skin fibroblasts derived from the same patients. Int J Radiat Biol 1993;63:191–8.
12. Nagashima Y, Ohaki Y, Tanaka Y, et al. Establishment of an epithelioid malignant schwannoma cell line (YST-1). Virchows Arch B Cell Pathol Incl Mol Pathol 1990;59:321–7.
13. Perry A, Roth KA, Banerjee R, Fuller CE, Gutmann DH. NF1 deletions in S-100 protein-positive and negative cells of sporadic and neurofibromatosis 1 (NF1)-associated plexiform neurofibromas and malignant peripheral nerve sheath tumors. Am J Pathol 2001;159:57–61.
14. DeClue JE, Heffelfinger S, Benvenuto G, et al. Epidermal growth factor receptor expression in neurofibromatosis type 1-related tumors and NF1 animal models. J Clin Invest 2000;105:1233–41.
15. Menon AG, Anderson KM, Riccardi VM, et al. Chromosome 17p deletions and p53 gene mutations associated with the formation of malignant neurofibrosarcomas in von Recklinhausen neurofibromatosis. Proc Natl Acad Sci U S A 1990;87:5435–9.
16. Legius E, Dierick H, Wu R, et al. TP53 mutations are frequent in malignant NF1 tumors. Genes Chromosomes Cancer 1994;10:250–5.
17. Mawrin C, Kirches E, Boltze C, Dietzmann K, Roessner A, Schneider-Stock R. Immunohistochemical and molecular analysis of p53, RB, PTEN in malignant peripheral nerve sheath tumors. Virchows Arch 2002;440:610–5.
18. Watson MA, Perry A, Tihan T, et al. Gene expression profiling reveals unique molecular subtypes of neurofibromatosis type 1-associated and sporadic peripheral nerve sheath tumors. Brain Pathol 2004;14:297–303.
19. Rosenbaum T, Rosenbaum C, Winner U, Muller HW, Lenard HG, Hanemann CO. Long-term culture and characterization of human neurofibroma-derived Schwann cells. J Neurosci Res 2000;61:524–32.
20. Upadhyaya M, Han S, Consoli C, et al. Characterization of the somatic mutational spectrum of the neurofibromatosis type 1 (NF1) gene in neurofibromatosis patients with benign and malignant tumors. Hum Mutat 2004;23:134–46.
21. Wang X, Ling MT, Guan XY, et al. Identification of a novel function of TWIST, a bHLH protein, in the development of acquired Taxol resistance in human cancer cells. Oncogene 2004;23:474–82.
22. Lee MS, Lowe GN, Strong DD, Wergedal JE, Glackin CA. TWIST, a basic helix-loop-helix transcription factor, can regulate the human osteogenic lineage. J Cell Biochem 1999;75:566–77.
23. Irizarry RA, Bolstad BM, Collin F, Cope LM, Hobbs B, Speed TP. Summaries of Affymetrix GeneChip probe level data. Nucleic Acids Res 2003;31:e15.
24. Castanon I, Baylies MK. A Twist in fate: evolutionary comparison of Twist structure and function. Gene 2002;287:11–22.
25. Reynolds JE, Fletcher JA, Lytle CH, Nie L, Morton CC, Diehl SR. Molecular characterization of a 17q11.2 translocation in a malignant schwannoma cell line. Hum Genet 1992;90:450–6.
26. Wu R, Lopez-Correa C, Rutkowski JL, Baumbach LL, Glover TW, Legius E. Germline mutations in NF1 patients with malignancies. Genes Chromosomes Cancer 1999;26:376–80.
27. Kourea HP, Orlow I, Scheithauer BW, Cordon-Cardo C, Woodruff JM. Deletions of the INK4A gene occur in malignant peripheral nerve sheath tumors but not in neurofibromas. Am J Pathol 1999;155:1855–60.
28. Birindelli S, Perrone F, Oggionni M, et al. Rb and TP53 pathway alterations in sporadic and NF1-related malignant peripheral nerve sheath tumors. Lab Invest 2001;81:833–44.
29. Berner JM, Sorlie T, Mertens F, et al. Chromosome band 9p21 is frequently altered in malignant peripheral nerve sheath tumors: studies of CDKN2A and other genes of the pRB pathway. Genes Chromosomes Cancer 1999;26:151–60.
30. Perry A, Kunz SN, Fuller CE, et al. Differential NF1, p16, and EGFR patterns by interphase cytogenetics (FISH) in malignant peripheral nerve sheath tumor (MPNST) and morphologically similar spindle cell neoplasms. J Neuropathol Exp Neurol 2002;61:702–9.
31. Ryan JJ, Klein KA, Neuberger TJ, et al. Role for the stem cell factor/KIT complex in Schwann cell neoplasia and mast cell proliferation associated with neurofibromatosis. J Neurosci Res 1994;37:415–32.
32. Markey MP, Angus SP, Strobeck MW, et al. Unbiased analysis of RB-mediated transcriptional repression identifies novel targets and distinctions from E2F action. Cancer Res 2002;62:6587–97.
33. Kastan MB, Zhan Q, el-Deiry WS, et al. A mammalian cell cycle checkpoint pathway utilizing p53 and GADD45 is defective in ataxia-telangiectasia. Cell 1992;71:587–97.
34. Ochi K, Mori T, Toyama Y, Nakamura Y, Arakawa H. Identification of semaphorin3B as a direct target of p53. Neoplasia 2002;4:82–7.
35. Lo PK, Chen JY, Lo WC, et al. Identification of a novel mouse p53 target gene DDA3. Oncogene 1999;18:7765–74.
36. Ross DT, Scherf U, Eisen MB, et al. Systematic variation in gene expression patterns in human cancer cell lines. Nat Genet 2000;24:227–35.
37. Nagayama S, Katagiri T, Tsunoda T, et al. Genome-wide analysis of gene expression in synovial sarcomas using a cDNA microarray. Cancer Res 2002;62:5859–66.
38. Maestro R, Dei Tos AP, Hamamori Y, et al. Twist is a potential oncogene that inhibits apoptosis. Genes Dev 1999;13:2207–17.
39. Yang J, Mani SA, Donaher JL, et al. Twist, a master regulator of morphogenesis, plays an essential role in tumor metastasis. Cell 2004;117:927–39.
40. Sosic D, Richardson JA, Yu K, Ornitz DM, Olson EN. Twist regulates cytokine gene expression through a negative feedback loop that represses NF-κB activity. Cell 2003;112:169–80.
41. Kwok WK, Ling MT, Lee TW, et al. Up-regulation of TWIST in prostate cancer and its implication as a therapeutic target. Cancer Res 2005;65:5153–62.
42. Nielsen GP, Stemmer-Rachamimov AO, Ino Y, Moller MB, Rosenberg AE, Louis DN. Malignant transformation of neurofibromas in neurofibromatosis 1 is associated with CDKN2A/p16 inactivation. Am J Pathol 1999;155:1879–84.
43. Lowe SW, Sherr CJ. Tumor suppression by Ink4a-Arf: progress and puzzles. Curr Opin Genet Dev 2003;13:77–83.
44. Kurtz A, Schulte AM, Wellstein A. Pleiotrophin and midkine in normal development and tumor biology. Crit Rev Oncog 1995;6:151–77.
45. Su W, Sin M, Darrow A, Sherman LS. Malignant peripheral nerve sheath tumor cell invasion is facilitated by Src and aberrant CD44 expression. Glia 2003;42:350–8.
46. Su W, Gutmann DH, Perry A, Abounader R, Laterra J, Sherman LS. CD44-independent hepatocyte growth factor/c-Met autocrine loop promotes malignant peripheral nerve sheath tumor cell invasion *in vitro*. Glia 2004;45:297–306.
47. Peirano RI, Goerich DE, Riethmacher D, Wegner M. Protein zero gene expression is regulated by the glial transcription factor Sox10. Mol Cell Biol 2000;20:3198–209.
48. Levy P, Vidaud D, Leroy K, et al. Molecular profiling of malignant peripheral nerve sheath tumors associated with neurofibromatosis type 1, based on large-scale real-time RT-PCR. Mol Cancer 2004;3:20.
49. Cheung M, Briscoe J. Neural crest development is regulated by the transcription factor Sox9. Development 2003;130:5681–93.
50. Oliver TG, Wechsler-Reya RJ. Getting at the root and stem of brain tumors. Neuron 2004;42:885–8.

Large-Scale Molecular Comparison of Human Schwann Cells to Malignant Peripheral Nerve Sheath Tumor Cell Lines and Tissues

Shyra J. Miller, Fatima Rangwala, Jon Williams, et al.

Cancer Res 2006;66:2584-2591.